Professional paper

Received: November 30, 2013
Accepted: March 26, 2014

A review of stratigraphic surfaces generated from multiple electrical sounding and profiling

Prikaz sekvenčnih stratigrafskih površin, pridobljenih z geoelektričnim sondiranjem in profiliranjem

Kamaldeen Omosanya[1,*], Akinwale Akinmosin[2], Jonathan Balogun[2]
[1]Olabisi Onabanjo University, Department of Earth Sciences, Ago-Iwoye, Nigeria
[2]University of Lagos, Department of Geoscience, Akoka, Nigeria
*Corresponding author. E-mail: kamaloomosanya@yahoo.com

Abstract

In this work, we investigate the accuracy of stratigraphic surfaces derived from multiple electrical sounding and traversing. Eight (8) VES stations with *AB*/2 of > 80 m each and three (3) Wenner profiling of > 120 m each were used for this investigation. The three principal surfaces interpreted include conglomeratic sand (top layer), sandstone (presumably compacted) and clayey sandstone. These rocks are correlated to the Ise Formation of eastern Dahomey Basin. Our result shows that widely-spaced VES are error-prone and may result in misinterpretation of subsurface resistivity and rock boundaries. Smaller spacing between VES stations can effectively detect minute resistivity anomalies. On the other hand, the inversion method used for interpretation of profiling data can influence the final resistivity values. We propose the criteria for generating stratigraphic surfaces to include (a) adequate geological mapping (b) small electrode spacing for profiling (c) closely-spaced VES stations and profiling lines (d) interpolation of thickness and resistivity in multiple direction and (e) the use of drill hole logs to tie VES models.

Key word: stratigraphic surfaces, VES, profiling, Ise

Izvleček

V članku opisujemo natančnost stratigrafskih površin, ki jih konstruiramo z geoelektričnim sondiranjem in profiliranjem. V ta namen smo uporabili podatke osmih točk vertikalnega električnega sondiranja (VES) z *AB*/2 > 80 m s Schlumbergerjevo elektrodno razporeditvijo in podatke treh profilov dolžine > 120 m z Wennerjevo elektrodno razporeditvijo. Iz podatkov geoelektričnega sondiranja in profiliranja smo interpretirali tri osnovne tipe kamnin, ki vključujejo konglomeratni pesek (zgornja plast), peščenjak (pretežno sprijet), zaglinjen peščenjak in preperelo podlago. Ti trije tipi ustrezajo enotam v Isa-formaciji iz Abeokuta skupine vzhodnega Dahomejskega bazena. Naši rezultati kažejo, da ima redka razporeditev VES-točk lahko za posledico napačno določitev električnih upornosti in s tem nepravilno določitev geoloških meja. Z manjšimi razdaljami med sondami lahko učinkovito zaznamo tudi majhne upornostne anomalije. Problem 2D-profiliranja je inverzna metoda modeliranja in kot posledica tega tudi doseg preiskav. Predlagamo nekaj meril za konstruiranje stratigrafskih površin, ki naj vključujejo (a) ustrezno geološko kartiranje, (b) majhne medelektrodne razdalje za profiliranje, (c) gosto razporeditev VES-točk in prečnih profilov, (d) interpolacijo debelin in električnih upornosti v več smereh in (e) uporabo podatkov vrtin, na katere navežemo VES-modele.

Ključne besede: sekvenčne stratigrafske površine, geoelektrično sondiranje, geoelektrično kartiranje, Ise

Introduction

Resistivity geophysical survey is one of the oldest and cheapest method of investigating subsurface electrical property and resistivity variation[1, 2]. Resistivity method is used to solve a wide variety of groundwater problems which include determination of zones with high yield potential in an aquifer e.g.[3, 4], leechate and other groundwater contamination e.g.[5, 6], determination of the boundary between saline and fresh water zones[7, 8], exploration of geothermal reservoirs[9, 10], and estimation of hydraulic conductivity and transmissivity of aquifer[11].

Sounding is one dimensional (1D) in nature providing subsurface information at a single point on the ground e.g.[12]. Contrastingly, profiling is two dimensional (2D) data providing a cross section beneath the Earth's surface unlike 3D data that image the geology as a volume[13]. Three dimensional methods are unique in that they provide better resolution and visualization[14, 15]. Hence, the earth volume can be displayed in depth (cm, m, km) and $x - y$ coordinates system[16, 17]. Planning 3D surveys could be laborious and expensive, often involving the design of appropriate line geometry for source (current electrode) and receiver (potential electrode) locations. To achieve this, a rectangular grid comprising of a line at least approximately along the line of steepest descent down the structure and another along a contour line on the structure is required *cf.*[18]. This is the general practice in 3D geophysical surveying *cf.*[19, 20]. Initial knowledge of the structure from surface or regional geology, satellite imagery, previous geophysical surveys such as gravity and magnetic is crucial for successful survey planning and design[19, 20].

The practice of generating shallow stratigraphic surfaces from multiple 1D or 2D resistivity data is budding in less developed countries. This is consequent to the sparse availability of equipment and knowledge appropriate to conduct 3D and 4D surveys[21]. Stratigraphic surfaces obtained through such practices are error prone and may result in misinterpretation of geological features and its associated resources.

The aim of this study is to validate the accuracy of stratigraphic surfaces generated from multiple sounding and profiling, an important piece of information for precise delineation of stratigraphic boundaries and subsurface resources. We hope to provide adequate information that will bridge the gap between constructed stratigraphic surfaces and those generated from real 3D surveys. The paper starts with a general overview of the regional geology. Description of geophysical methods which include electrical sounding and profiling along specific surveys lines follows. In the discussion we reappraise the techniques and their relevance to the current study and eventually provide criteria for generating realistic stratigraphic surfaces.

Regional Geologic Setting and Stratigraphy

The study area is located east of the West African Craton (WAC) (Figure 1). The Dahomey basin constitute part of a system of West African peri-cratonic basin developed during Late Jurassic to Early Cretaceous rifting associated with the opening of the Gulf of Guinea[22–25]. The crustal separation and thinning was accompanied by an extended period of thermally induced basin subsidence through the Middle – Upper Cretaceous to Tertiary as the South American and the African plates entered a drift phase[26, 27]. The Ghana Ridge, presumably an offset extension of the Romanche Fracture Zone, and the Benin Hinge Line, a bedrock escarpment which separates the Okitipupa structure from the Niger Delta basin are located on the western and eastern boundaries of the Dahomey basin. The Benin Hinge Line is the continental extension of the Chain Fracture Zone.

The onshore part of the basin covers a broad arc-shaped belt profile of ~600 km^2 in extent. The onshore section attains a maximum width along its N-S axis, ~130 km around the Nigerian – Republic of Benin border. The basin narrows to ~50 km on the eastern side where the bedrock assumes a convex upwards outline with concomitant thinning of sediments. Notably, along the north eastern fringe of the basin where it rims the Okitipupa high is a brand of tar (oil) sands and bitumen seepages[28]. The eastern Dahomey basin has been investigated specifically for its oil sand resource[29].

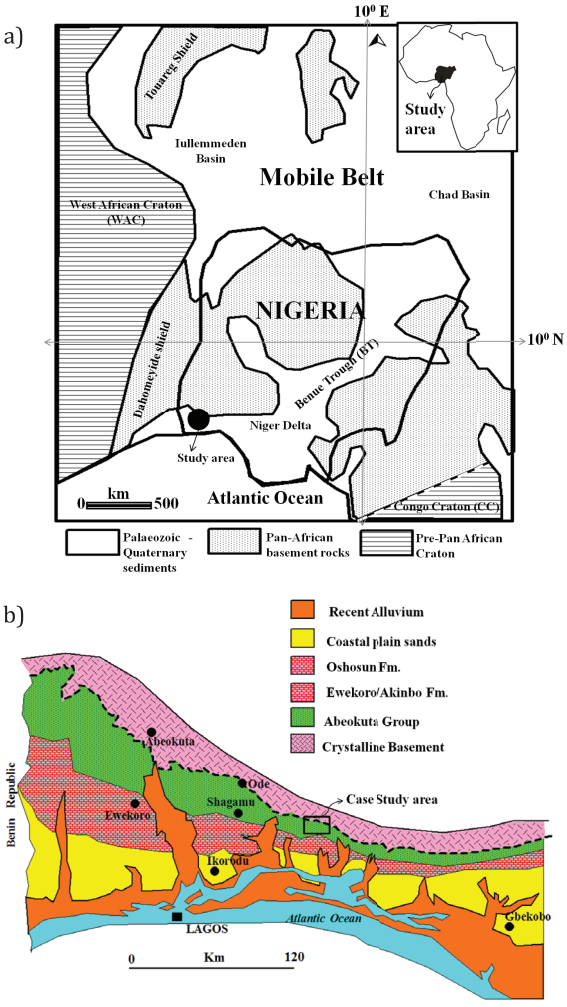

Figure 1: *a) Regional geological map of Nigeria in the context of West African and Congo Craton (modified after[30]). b) Simplified Geological map of the study area and environs. The geological boundary between the crystalline bedrock and sedimentary rock is shown with thick broken line. Further litho and chrono stratigraphic division of the study area is provided in Table 1.*

The lithostratigraphic units of the case study area are summarised in Figure 1b and Table 1. The area belongs to the Ise Formation of the Cretaceous Abeokuta group which is the oldest and the thickest group of sediment in the Dahomey basin[31, 32]. The Abeokuta group is composed of the Ise, Afowo and Araromi Formation. Ise Formation unconformably overlies the bedrock complex of Southwestern Nigeria. This unit consists of conglomerates, grits, coarse to medium grained sands interbedded with kaolinite. The conglomerates are imbricated and composed of ironstones at some localities[33]. An age range of Neocomian-Albian is assigned to this Formation based on paleontological assemblages[32].

The Afowo Formation comprises coarse to medium grained sandstone with variable but thick interbedded shale, siltstone and claystone. The sandy facies are tar-bearing while the shales are organic-rich[34]. Using palynological assemblage, a Turonian age is assigned to the Lower part of this Formation, while the upper part ranges into Maastrichian. The youngest Cretaceous Formation in the group is Araromi Formation which is composed of fine-medium grained sandstone, shales, siltstone with interbedded limestone, marl and lignite.[32] assigned a Maastrichian to Palaeocene age to this formation based on faunal content.

The Abeokuta group is overlain by the Imo group (Ewekoro and Akinbo Formation[31, 33, 35, 36], the Oshosun Formation[31, 33], Coastal plain sands and recent alluvium[31].

Table 1: *The stratigraphic units of eastern Dahomey basin*

Jones and Hockey (1964)[31]			Omatsola and Adegoke (1981)[32]		Agagu (1985)[36]	
	Age	**Formation**	**Age**	**Formation**	**Age**	**Formation**
Quaternary	Recent	Alluvium			Recent	Alluvium
Tertiary	Pleistocene- Oligocene Eocene Palaeocene	Coastal Plain Sand Ilaro Ewekoro	Pleistocene- Oligocene Eocene Palaeocene	Coastal Plain Sand Ilaro Oshosun Akinbo Fm	Pleistocene- Oligocene Eocene Palaeocene	Coastal Plain Sand Ilaro Oshosun Akinbo Ewekoro
Cretaceous	Late Senonian	Abeokuta	Maastrichtian- Neocomian	Araromi Afowo Ise	Maastrichtian- Neocomian	Araromi Afowo Ise
Precambrian Crystalline Bedrock Rocks						

Methods

Resistivity surveys including three (3) profiling lines and eight (8) vertical electrical sounding (VES) were done over an area of ~56 400 m^2. The sounding involves application of artificial electrical field method where electrode spacing is increased along traverse lines to obtain subsurface information at a given location (the survey layout is shown in Figure 3). The greatest limitation of electrical resistivity sounding method is that it does account greatly for lateral changes in the subsurface resistivity[1]. For a more accurate result of the subsurface model, a two dimensional (2D) model where the resistivity changes in vertical and horizontal direction along the survey line was incorporated with the vertical electrical sounding. In this case, it was assumed that resistivity does not change in the direction perpendicular to the survey line. This method also finds its usefulness in the area of moderately complex geology[13]. The ohmmeter resistivity meter used for the research measures resistance based on Ohm's law for current (I), voltage (V) and resistance (R) (Figure 2).

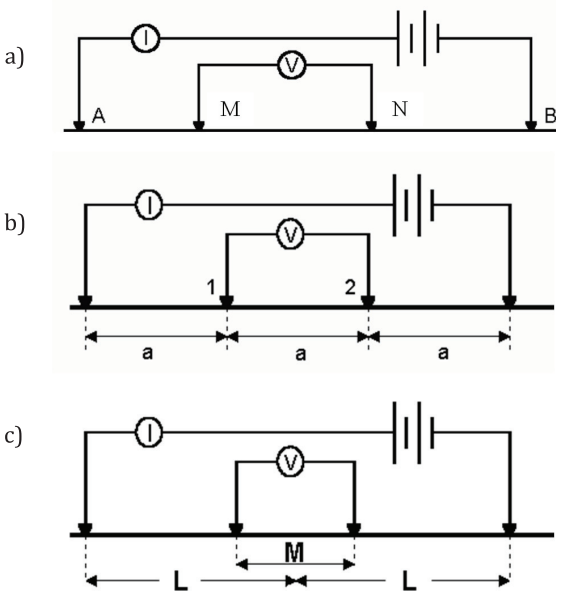

Figure 2: *a) General electrode configuration for electrical geophysical method; b) Wenner array configuration, c) Schlumberger array configuration.*

Sounding

The VES uses the principle of wider current electrode separation offers deeper current penetration and depth probe e.g.[8, 37]. Hence, apparent resistivity values observed at larger separations are governed by the resistivity of deeper layers[38, 2]. Current was injected into the earth through two electrodes (A and B) and the resulting voltage differences were measured at two potential electrodes (M and N). Hence, an apparent resistivity (ρ_a) values at each separation can be calculated using the general relation, $\rho_a = KV/I = KR$[39]. Electrode configuration of $AB \geq 5\,MN$ was maintained except with the initial values of current and potential electrodes spacing of $AB/2$ = 1.0 m and $MN/2$ = 0.25 m. The electrode layout for the sounding is shown in Figure 2c.

K is the array geometric factor and is defined as $K = \pi/2l\,(L^2 - l^2)$, where L is $AB/2$, l is $MN/2$; current (I) and voltage (V) values, and the geometric factor (K) depends on the arrangement of the four electrodes. For this study, Schlumberger array was used for the sounding. The resistivity measurement for each $AB/2$ and corresponding $MN/2$ separations are shown below:

$AB/2$ = 1, 2, 3, 4, 6, 6, 9, 12, 15, 15, 20, 25, 32, 40, 40, 50, 65, 80, 100 and

$MN/2$ = 0.25, 0.25, 0.25, 0.25, 0.25, 0.5, 0.5, 0.5, 0.5, 1, 1, 1, 1, 1, 2.5, 2.5, 2.5, 2.5, 2.5.

The apparent resistivities (ρ_a) were plotted against the electrode spacing ($AB/2$) in order to obtain a resistivity-depth model for iteration on the WINRESIST software. The best iterations were obtained at RMS error of < 5 %. The depth, thickness and resistivity of the geoelectric layers were estimated and used to build 2D and 3D resistivity tomogram for the area.

Profiling

The profiling involve constant separation technique (CST) using the Wenner electrode configuration. Three (3) profile lines ~120 m long were chosen along the less rugged portion of the survey area (Figure 3). Subsequently, the profiles lines were separated ~20 m in the N – S direction to give better resolution of the subsurface resistivity variation. A current of 5 mA was introduced into the ground and the mean resistivity value

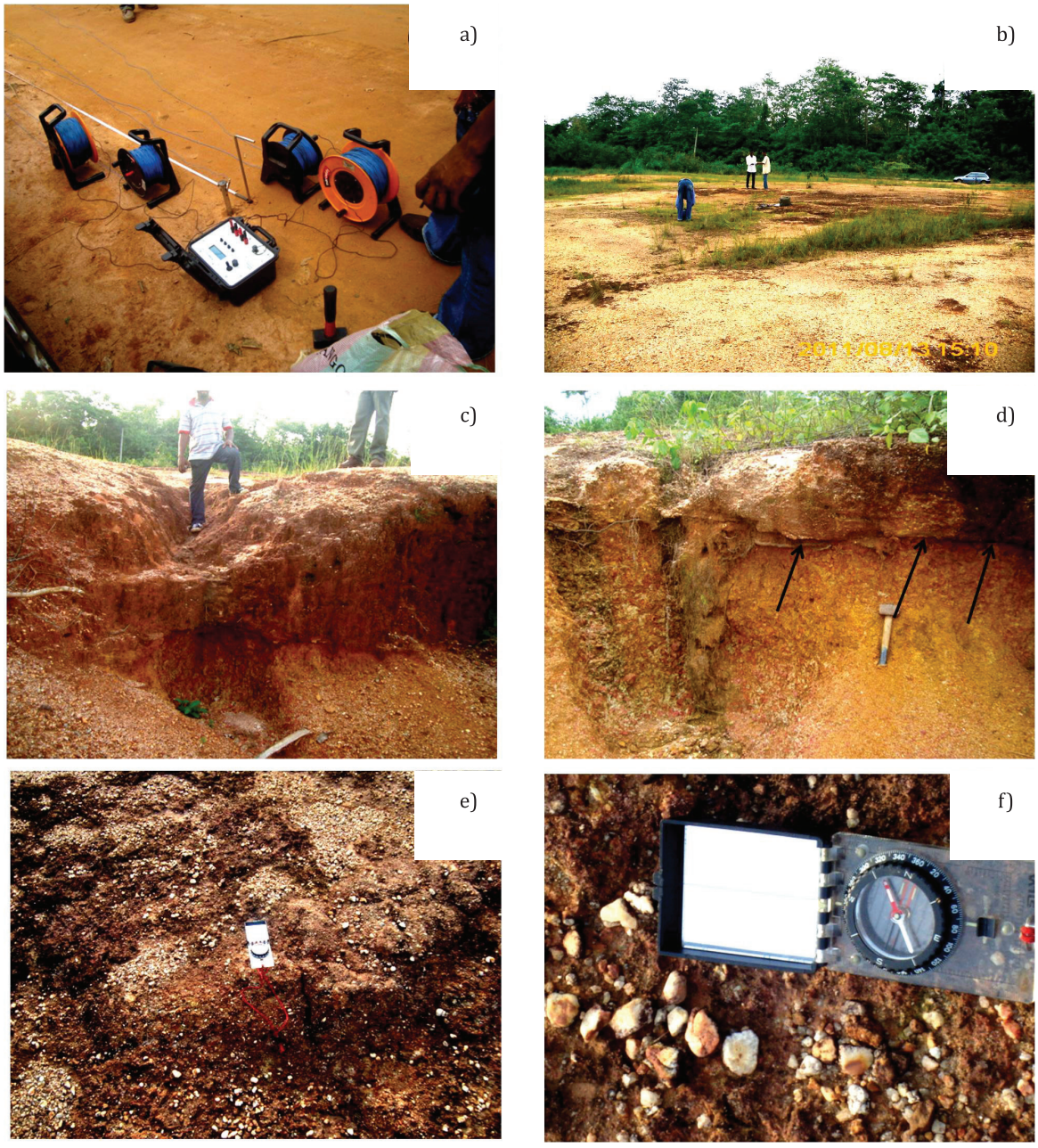

Figure 3: *a) The survey layout for the electrodes; b) The survey area where both profiling and sounding were carried out. The topography is nearly horizontal and the rocks are characterised by angle of dip of < 1°; c) cross section through the subcrop; d)–e) Outcrop of conglomeratic sandstone, the bedding plane between the conglomeratic sands and sandstone is nearly horizontal; f) Clasts of sandstone found in the conglomeratic sandstone are sub-rounded to very well-rounded.*

over four cycles was obtained. As the distance between the current electrodes was progressively increased, the position of the potential electrode remained unchanged until the voltages were too small to be measured. The electrode spacing between adjacent electrode was assigned "*a*". Hence, for a system with 20 electrodes, there are (20 – (1 × 3)), (20 – (2 × 3)), (20 – (3 × 3)), (20 – (4 × 3)) possible measurements for "1*a*", "2*a*", "3*a*", "4*a*" respectively and so on. This implies that, as the electrode spacing increases, the number of measurement decreases.

The first procedure was to carry out all the possible measurements for the Wenner array with electrodes spacing of "1*a*". For the first measurement, electrodes 1 to 4 were as A, M, B and N respectively. The positions of these electrodes were changed according to increasing number of elec-

trode spacing for "1*a*". The same technique was repeated for "2*a*", "3*a*", "4*a*", "5*a*"and "6*a*" spacing. The profiling was done with the practical assumption that depths of (3, 6, 9, 12, 15 and 18) m were being investigated (depth is ~0.6 of electrode spacing). The electrode layout for Wenner is shown in Figure 2b.

Resistivity values derived from the survey were converted to apparent resistivities using the geometric factor for Wenner; the data were processed on Excel spreadsheet and RES2DINV ver 3.55 software. Smooth and robust inversions were done to compare results and detect sedimentary boundaries. The inversion pro-

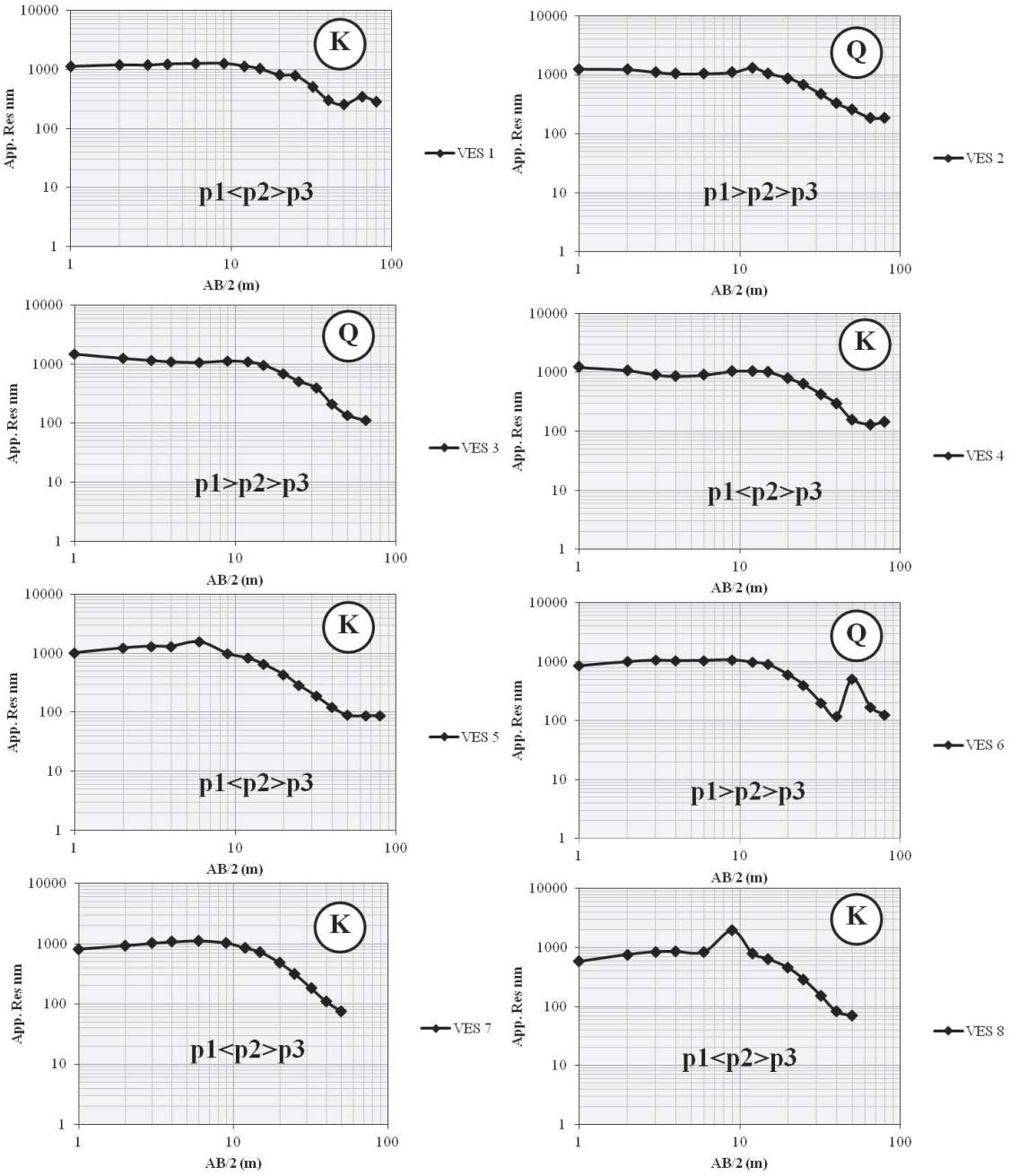

Figure 4: *The resistivity plot for the VES stations were done from direct field measurements. The AB/2 versus apparent resistivity shows that the subsurface is multi-layered and composed of three rock types characterised as K- and Q-type curves.*

cess is iterative, and useful for creating resistivity models of the subsurface[38, 14]. A starting model was chosen based on a-priori information from ground truth or averaged geophysical measurements; apparent resistivity data was modelled according to the survey geometry. The calculated data were compared with the field measurements and the model updated to accommodate the difference between the observed and estimated results. This procedure was repeated until the derived data matched the actual readings to within an interpreter defined level of error[40]. The consequence of the inversion process is a better estimate of depth for cross section plots, which turns resistivity pseudo sections into reliable approximations of the subsurface variation.

Interpolation resistivity and thickness of the layers

Estimated thickness and resistivity of three principal rock types were interpolated across the position of the VES stations and the profile lines to generate cross sections and 3D tomogram (Figures 5 and 6). The *x* and *y* direction include longitude and latitude of the stations and positions at every 20 m along each of the traverse, z-value is the thickness of the layers estimated. The stratigraphic thickness (isopach) maps were produced on Surfer 8 (Figures 6 and 8).

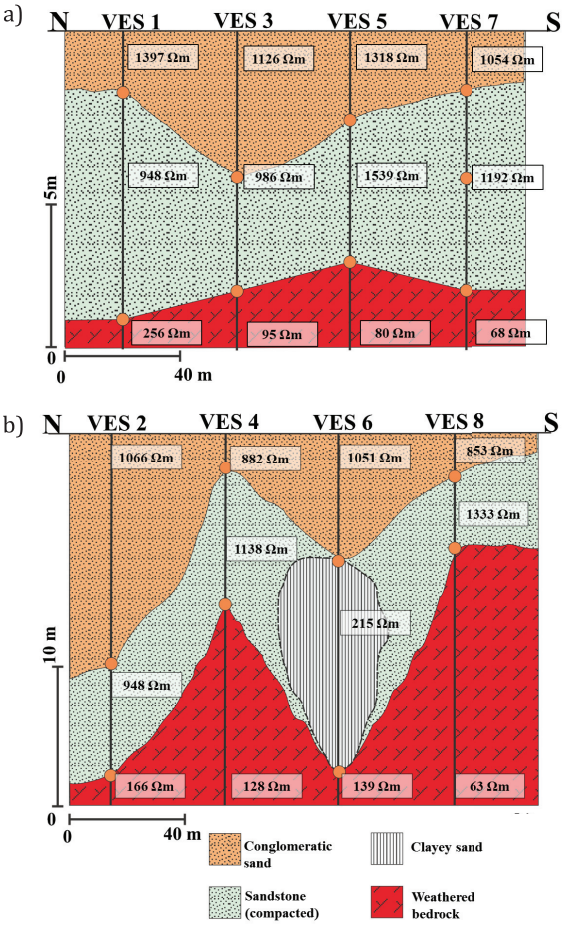

Figure 5: *Cross section through the study area. Thicknesses and resistivities of the geoelectrical section were interpolated from multiple VES models which include a) VES 1, 3, 5, & 7 and b) VES 2, 4, 6, & 8. The sections revealed exaggerated angle of dip and strata geometries for the three rock types. The weathered bedrock is characterised by comparatively low apparent resistivity suggestive of high clay content.*

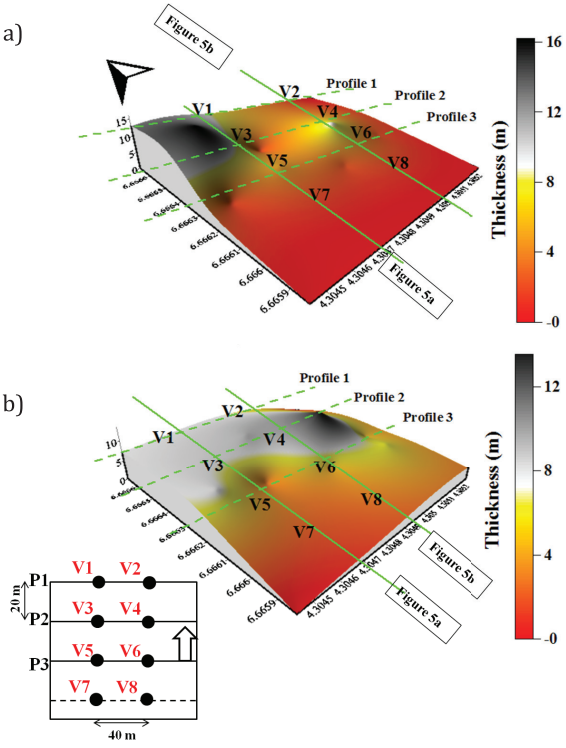

Figure 6: *Isopach map for a) conglomeratic sand b) sandstone. The highest thicknesses are recorded in the NW region of the study area corroborating the result of Figure 8. The isopach maps were produced by interpolating the thicknesses of both rock types across the VES stations. N.B: The numbered circles correspond to the position of VES 1 to 8. Inset: The survey layout.*

Results

In the following section the result from the survey is presented in phases such as the vertical electrical sounding, 2D models, and stratigraphic surfaces/3D models. These sections are followed by a discussion on the accuracy of the geological boundaries obtained from both results.

Geo-electric layers from Vertical Electrical Sounding

The plots of apparent resistivity against electrode spacing AB/2 are indicative of 3-layered stratigraphy. The curves are K and Q curves (Figure 4). The four (4) lithology units include conglomeratic sand (topmost stratum at all VES station), sandstone (presumably compacted), clayey sandstone and weathered bedrock. These units have resistivity values of 853–1 397 Ω m, 948–1 539 Ω m, 215 Ω m and 63–256 Ω m and thickness of 2–16 m, 4–14 m, 14 m and infinity respectively (Figure 5 and Table 2). The inferred weathered bedrock occurs at depth of ~8 m to ~24 m at all the VES stations. The clayey sand was detected beneath VES 6 only and apparently represents a different sandstone facies from the compacted sandstone and sandstone found at other VES points (Figure 5 and Table 2).

Table 2: *Parameters determined from the VES points*

VES No	No of Layers	Depth	Thickness	Resistivity	Lithology
1	3	0–2	2	1 397	Conglomeratic Sand
		2–10	8	948	Sandstone
		10–∞		256	Weathered Bedrock
2	3	0–16	16	1 066	Conglomeratic Sand
		16–24	8	948	Sandstone
		24–∞		166	Weathered Bedrock
3	3	0–5	5	1 126	Conglomeratic Sand
		5–9	4	986	Sandstone
		9–∞		95	Weathered Bedrock
4	3	0–2	2	882	Conglomeratic Sand
		2 –12	10	1 138	Sandstone
		12–∞		128	Weathered Bedrock
5	3	0–3	3	1 318	Conglomeratic Sand
		3–8	5	1 539	Sandstone
		8–∞		80	Weathered Bedrock
6	3	0–9	9	1 051	Conglomeratic Sand
		9–23	14	215	Clayey Sand
		23–∞		139	Weathered Bedrock
7	3	0–2	2	1 054	Conglomeratic Sand
		2–9	7	1 192	Sandstone
		9–∞		68	Weathered Bedrock
8	3	0–3	3	853	Conglomeratic Sand
		3–8	5	1 333	Sandstone
		8–∞		63	Weathered Bedrock

Electrical Reflection Coefficient

In order to validate resistivity anisotropy across layers and boundary condition of the interpreted intervals, an estimate of the electrode reflection coefficient, k was calculated along the interfaces of the different rock types using equation 1

$$k = \left(\frac{\rho 1 - \rho 2}{\rho 1 + \rho 2}\right) \quad (1)$$

k is electrical reflection coefficient
$\rho 1$ = apparent resistivity of the first layer
$\rho 2$ = apparent resistivity of the second layer

The k between conglomeratic sand and sandstone is –0.1 across VES point 4, 5, and 7. Across VES 2 and 3 k between those two lithological units is 0.1, and for VES 1 and 8 k is 0.2 and –0.2 accordingly (Table 3). This suggests that the coefficient is relatively consistent across some of the VES points. However, at VES 6, the k value between the conglomeratic sand and clayey sand is 0.7, suggesting a high degree of dissimilarity between these lithology types. Furthermore, the k value between the weathered bedrock and sandstone at VES points 1, 2, 3, 4, 5, 7 and 8 ranges from 0.7 to 0.9 (Table 3).

Table 3: *Electrical reflection coefficient across the interpreted interfaces*

VES No	Res. Point	Resistivity	Lithology	Electrical reflection coefficient
1	p1	1 397	Conglomeratic Sand	0.2
	p2	948	Sandstone	0.6
	p3	256	Weathered Bedrock	
2	p1	1 066	Conglomeratic Sand	0.1
	p2	948	Sandstone	0.7
	p3	166	Weathered Bedrock	
3	p1	1 126	Conglomeratic Sand	0.1
	p2	986	Sandstone	0.8
	p3	95	Weathered Bedrock	
4	p1	882	Conglomeratic Sand	–0.1
	p2	1 138	Sandstone	0.8
	p3	128	Weathered Bedrock	
5	p1	1 318	Conglomeratic Sand	–0.1
	p2	1 539	Sandstone	0.9
	p3	80	Weathered Bedrock	
6	p1	1 051	**Conglomeratic Sand**	0.7
	p2	215	**Clayey Sand**	0.2
	p3	139	Weathered Bedrock	
7	p1	1 054	Conglomeratic Sand	–0.1
	p2	1 192	Sandstone	0.9
	p3	68	Weathered Bedrock	
8	p1	853	Conglomeratic Sand	–0.2
	p2	1 333	Sandstone	0.9
	p3	63	Weathered Bedrock	

In contrast, there is a strong similarity between the clayey sand and weathered bedrock at VES 6. This is evidenced by *k* value of 0.2 (Table 3). Overall, a high *k* suggests dissimilarity between rock types while a very low value implies homogeneity of rock types.

Resistivity cross section from 2D profiling

The apparent resistivity values for the profiling are described from the smooth inverted pseudo section. Profile 1 revealed three rock types which include conglomeratic sands with resistivity value of 386–1 065 Ω m, compacted ferruginised sandstone of > 1 065 Ω m, and weathered bedrock of < 386 Ω m (Figure 7). Contrastingly, the robust pseudo section shows dominance of compacted ferruginised sandstone having resistivity values of > 1 249 Ω m from the surface to depth of ~12 m. Other rock types include conglomeratic sands and weathered bedrock with resistivity value of 354–1 249 Ω m and < 354 Ω m respectively (Figure 7). Both pseudo sections show that the conglomeratic sands are sandwiched within the compacted ferruginised sandstone on the eastern side of profile 1. Equally, profile 2 shows a similar succession of rock types but with resistivity value of > 852 Ω m, 337–852 Ω m, and < 337 Ω m. At the uppermost and central section of profile 2, the conglomeratic sands are interbedded within the compacted ferruginised sandstone (Figure 7). However, the conglomeratic sands are predominant at the western to central uppermost section of profile 3, occurring to depth of ~12 m and ~5 m on the smooth and robust pseudo section respectively (Figure 8). To the eastern uppermost part, the compacted ferruginised sandstone occurs to depth of < 9 m. The resistivities of the rock types include > 1 019 Ω m, 277–1 019 Ω m and < 277 Ω m for compacted ferruginised sandstone, conglomeratic sands and weathered bedrock respectively.

Average resistivities for the three principal rock types are 150–1 000 Ω m, > 1 019 Ω m and < 400 Ω m (Figure 7). Field observation shows that weathered bedrock is composed of weathered clasts of feldspar apparently related to either porphyritic granite or porphyroblastic gneiss protolith. The degree of weathering is intense and the rock equivocally resembles a mudstone (Figure 3).

Stratigraphic surfaces from multiple VES and profiling

The isopach map in Figure 6 shows that conglomeratic sand is the thickest NW of the profile lines and thins to SW and SE. An anomalous high thickness of conglomeratic sand was identified ENE of the study area. Similarly, the sandstone is the thickest NE of the traverses where it is manifested expressed as a dome compared to thickness values in the surrounding (Figure 6). The thickness of sandstone in the NE is smaller than in the NW. The lowest thickness of the sandstone layer is recorded SW of profile lines (Figure 6).

The cross sections produced from VES data shows that conglomeratic sand is the thickest beneath VES 2 and relatively constant across VES 1, 5, & 7 which concur with the thickness trend observed in Figure 5. Furthermore, Figure 6 revealed similar variation in thickness for the sandstone layer when compared with Figure 8. The highest thickness of the sandstone beneath VES 6 is attributed with the presence of the clayey sand (Figure 5). It is important to note that profile line 3 crosses VES 5 and VES 6; both soundings are located at 40 m and 80 m mark of the profile line respectively. The three layers interpreted from the 2D profile are conglomeratic sand, sandstone and weathered bedrock with resistivity value of > 792 Ω m, 396–792 Ω m and < 396 Ω m, their thicknesses being ~9 m, ~4 m and infinity respectively. Two layers were interpreted under VES 6: they include the conglomeratic sand and the sandstone with resistivity value of > 792 Ω m and 560 Ω m respectively. When compared with the result from the VES points, the overlap between resistivities and depth values exist (see Figures 5, 6 and 8).

Discussion

The main purpose of resistivity surveys is to determine either the variation of resistivity with depth or estimate the lateral variations in resistivity associated with the presence of economic deposits, pollutants or tectonic structures[41–43]. The former reflect horizontal stratification of earth materials involving meas-

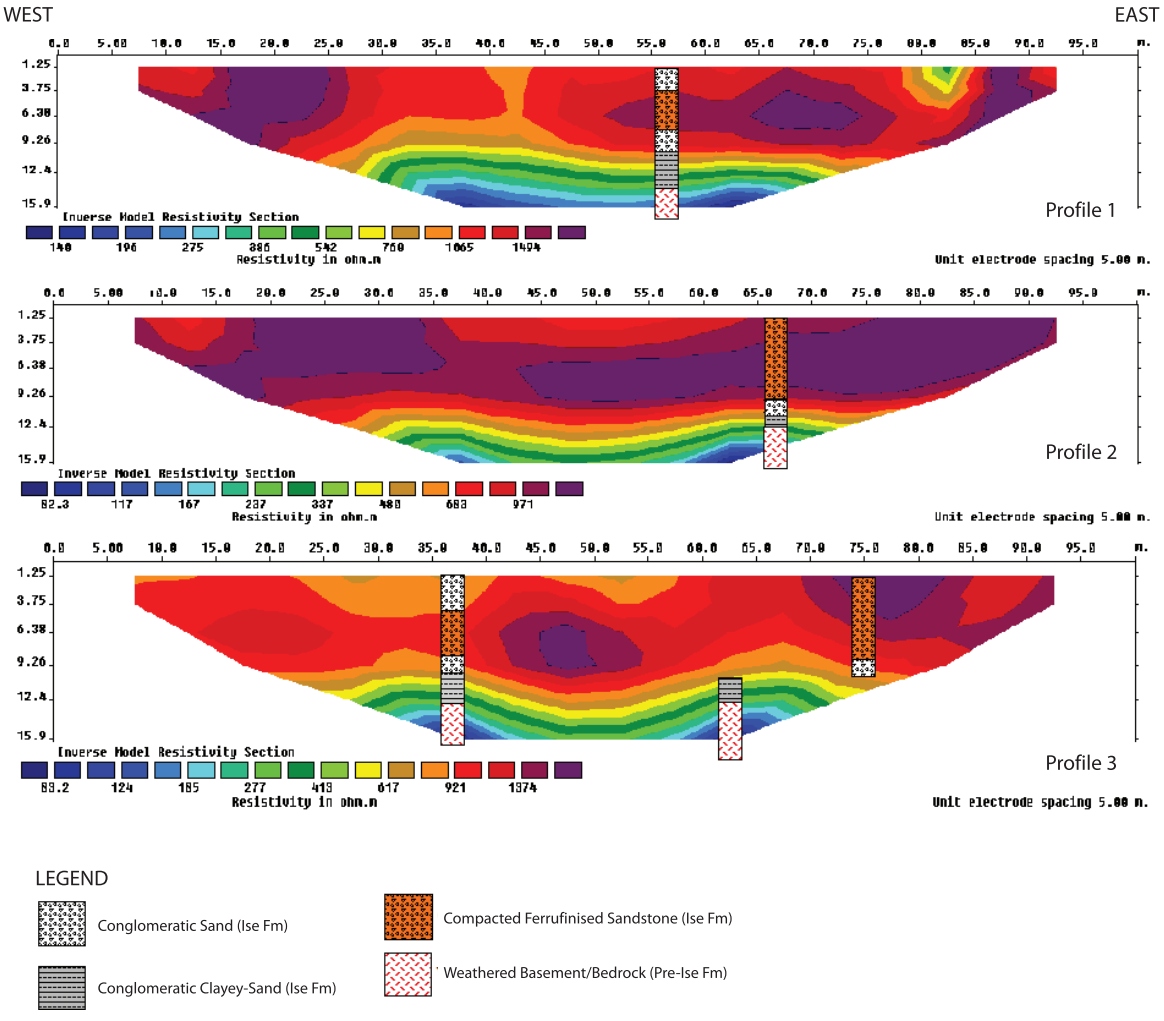

Figure 7: *The smooth inverted resistivity pseudo section along Profile 1, 2 and 3 from North to South. The principal lithology types include the conglomeratic sands, compacted ferruginised sandstone and the weathered bedrock with resistivity values of 150–1 000 Ωm, >1 019 Ωm and less than 400 Ωm respectively.*

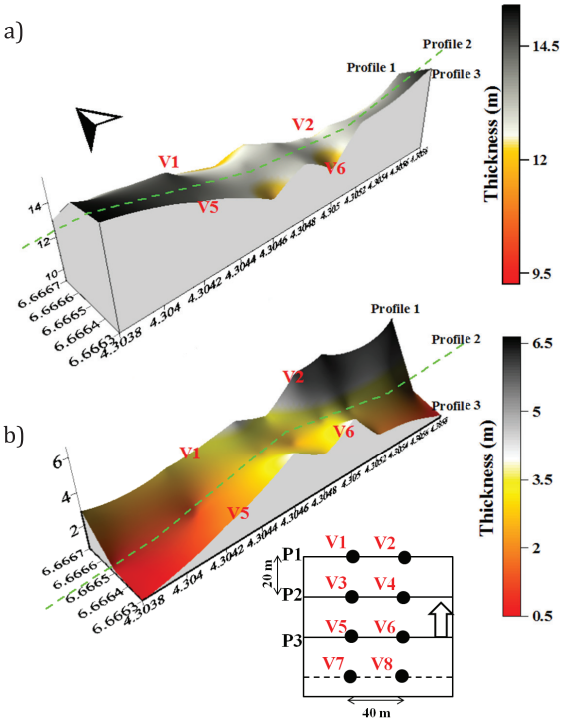

Figure 8: *a) Isopach map and cross section of the Ise Formation b) Cross section through the weathered bedrock/ basement. These figures are produced from interpolation of the 2D pseudo sections in Figure 7. The position of profile lines is from the north of Fig. 6 to the E-W broken line. N.B: The Ise Formation is sensu the conglomeratic sands and compacted ferruginised sandstone. The isopach map displays the thickness of the Ise to the top of the weathered basement, while the topography for the basal unit was estimated from the difference of the thickness of Ise Formation from the total depth shown on stratigraphic sections. Inset: The survey layout.*

urements of apparent resistivity at a single location with systematically varied electrode spacing. This procedure is called vertical electrical sounding (VES), or vertical profiling[44]. Surveys of lateral variations can be made at spot or along definite lines of traverse, a procedure called horizontal profiling or constant separation traversing (CST)[38, 40]. The greatest limitation of sounding is that it does not adequately account for horizontal variation in subsurface resistivity. Profiling or 2D models are more accurate but suffer the set back of limited depth of investigation. During profiling, the resistivity variation in both vertical and horizontal direction is modelled effectively especially for shallow depths. Therefore, using sounding and profiling to produce stratigraphic surfaces entail viewing the geology from different perspective yet with the goal of prodding similar result.

Array configuration and parameters are considerably dependent on the objective of the survey, available time and topography of the site[39]. To get the best subsurface information requires a well constrained survey with appropriate electrode configuration. This invariably affects data processing and the quality of interpretation model. The number of measurement is proportionate to electrode spacing and length of the survey traverse[38]. Schlumberger array allows the highest number of electrode spacing and survey length possible. Not only this, Schlumberger array provides for high signal-to-noise ratios, good resolution of horizontal layers, and good depth sensitivity[45]. An initial distance from the center of the array to either of the current electrodes is spacing *s*. Consequently, errors in apparent resistivity are within 2 % to 3 % if the distance between the potential electrodes does not exceed $2s/5$[46]. Potential electrode spacing is dependent on the minimum value of *s*. However, Wenner array is suited to smallest number of measurement but greater lateral resolution. In rugged topography, Wenner configuration electrode spacing is ineffective[40, 12].

Specifically, Wenner profiling in this study used initial a spacing of 5 m while the sounding were done starting with s value of 1 m for current electrodes. Hence, the maximum a spacing of 40 m can only yield depth of ~24 m while maximum current electrode spacing of 80 m can yield depth of < 40 m. It implies the depth of investigation is not consistent across both survey. To remove the ambiguity in depth requires running several VES prior the profiling. The exercise would provide a guide for the best electrode spacing needed for the 2D profiling. The resolution of the traverse line is governed by the fineness of the grid derived from initial VES parameter[39]. Therefore, combined vertical and horizontal methods may be used. If available drill hole logs at the sounding station can be used to effectively tie the lithology to their resistivity values.

Processing for both techniques is straight forward. Most resistivity meter are designed to measure resistance, the apparent resistivity value is derived from the product of the resistance with the appropriate geometric factor for the electrode configuration used. The caution during acquisition is to effectively monitor how

the potential diminishes with increasing current spacing. This will reduce error associated with underestimation of the geology during processing and interpretation of results. Again, this is dependent on the shrewdness of the geophysicist and his experience to increase the current appropriately. Of importance is the interval or cycles over which the resistance value is averaged. Averaging the resistance value in a cycle of 4 has proved very effective[21, 47].

The interpretation of sounding starts with plotting field measured apparent resistivity against electrode spacing in a diagram. The plot is a curve which is used to define initial geoelectrical model such as resistivities and thicknesses for each individual layer. Before the model could be defined, the plot is matched with standard master curves to obtain the best fit of layer parameters[38, 1, 2]. The initial model obtained is subsequently run over different commercial software and iterated at the least possible error. This procedure benefits greatly from the knowledge of local geology and the experience of the geophysicist. The greatest shortcoming of the direct interpretation pertains to electrical anisotropy at different depth and strata[1, 2]. Often the final geoelectrical sections are interpolated over several soundings to obtain cross section or a volume of the geology. For profiling, apparent resistivity values are plotted and contoured on maps or plotted as profiles. On the resistivity pseudo section, areas of anomalous values or patterns can be identified. 2D profiling integrates technique of 1D sounding along a survey line (i.e. 2D plane). The result is a contoured image, which displays the distribution of apparent resistivity values. In order to convert the apparent resistivity data to true resistivity, the data are inverted using either robust or smooth inversion, most often[48, 14].

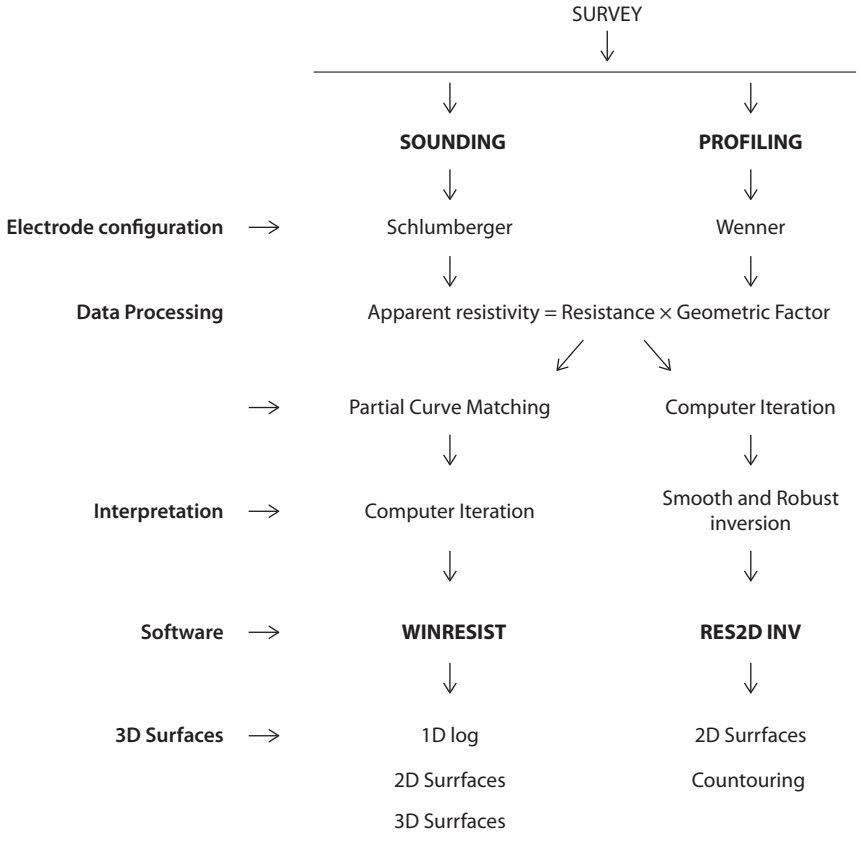

Figure 9: *Flowchart for comparing geoelectrical techniques of sounding and profiling as used in this work. Differences in results are related to the data processing technique and to acquisition parameters especially the direction of survey line and electrode spacing.*

Furthermore, stratigraphic surfaces were produced by interpolating thickness and resistivity in a grid of 40 m × 40 m in the N-S and E-W direction. This resulted in an overestimation of the geometry of the sections especially the angle of dip and strata geometry. Figure 5 shows that the Ise Formation is characterised by angle of dip > 1° which contradicts the observation made on the field. The actual dips of the Ise strata are < 1° as shown in Figure 3d. In addition, the clayey sand is shown as a lens within the compacted sandstone (Figure 5). These features were not picked by the profiles/resistivity pseudo sections. However, the location of the ferruginised sandstones lobes and lenses were adequately resolved despite the 2D section being oriented in N-S direction in contrast to E-W direction of the profiling lines. The surfaces interpolated from the profiling are rather closely spaced compared with the VES. Hence, the stratigraphic surface obtained from the profiling has better resolution and estimation of the stratigraphic geometry. The overlap between smooth and robust inverted pseudo sections shows that the geometry of the strata was effectively mapped. Robust inversion is useful for mapping complex geology and lap geometries[48]. Therefore, interpolation of geoelectrical section can be a fruitful exercise where the lateral continuity of strata is not geologically variable.

In order to reduce interpretation errors associated with electrical anisotropy, it is useful to estimate the electrical coefficient (Equation 1, Table 3). For the VES section, it provides hints on resistivity heterogeneity in the downhole direction. As it is often the case with VES, resistivity is higher perpendicular to layering e.g. bedding, foliation, lamination etc. rather than along layering[14]. In this work, electrical coefficients signify the presence of multi-layer geoelectrical section. High absolute k values are associated with very dissimilar lithology type. Hence, the k values from the VES corroborate the interpretation of the resistivity pseudo sections. However, determining the electrical coefficient over the profiles could be laborious.

Conclusion

In the absence of 3D equipments and methods for resistivity investigation in developing countries, this study has provided guideline for generating stratigraphic surfaces from available data acquired by multiple electrical sounding and profiling. In this work we showed that stratigraphic surfaces interpolated from the 1D and 2D data are reasonably similar in terms of thicknesses and resistivities of the layers. The maximum thickness of the Ise Formation estimated from both techniques is > 16 m. Resistivity values range from 900–1 300 Ω m. In addition, both techniques pointed to the presence of highly weathered clayey bedrock. However, the differences in results from both techniques are correlated to acquisition parameters such as the electrode spacing, distance between traverses and VES locations. Interpolation of VES data is very useful in an environment where the geology is simple and characterised by less variability. A combination of VES and CST array, such as a multi-level dipole-dipole array, can overcome the limitations associated with the both techniques. To generate effective stratigraphic surfaces, interpolation of resistivity and thickness along variable azimuth is required. Drill hole logs and advanced geological mapping could enhance the results obtained from these methods and consequently the representation of surfaces generated from them. Hence, the criteria for generating stratigraphic surfaces using sounding and profiling data should include advanced geological mapping, small electrode spacing, azimuthal interpolation combining both vertical and horizontal methods and adequate information from drill hole logging. A general comparison of both techniques is given in Figure 9.

Acknowledgement

We acknowledge comments and opinions of the anonymous reviewers. The understanding and support of Maryam, Aisha and Hawa during the preparation of the manuscript is remarkable.

References

[1] Kearey, P., Brooks, M., Hill, I. (2002): *An introduction to geophysical exploration*. Wiley- Blackwell.

[2] Telford, W., Geldart, L., Sheriff, R., Keys, D. (1976): *Applied geophysics*. Cambridge University Press.

[3] Sainato, C., Galindo, G., Pomposiello, C., Malleville, H., de Abelleyra, D., Losinno, B. (2003): Electrical conductivity and depth of groundwater at the Pergamino zone (Buenos Aires Province, Argentina) through vertical electrical soundings and geostatistical analysis. *J. South Am. Earth Sci*., 16, pp. 177–186.

[4] Shaaban, F. F. (2001): Vertical electrical soundings for groundwater investigation in Northwestern Egypt: a case study in a coastal area. *J. Afr. Earth Sci*., 33, pp. 673–686.

[5] Ariyo, S. O., Omosanya, K. O., Oshinloye, B. A. (2013): Electrical resistivity imaging of contaminant zone at Sotubo dumpsite along Sagamu-Ikorodu Road, Southwestern Nigeria. *Afr. J. Environ. Sci. Technol.,* 7, pp. 312–320.

[6] Reyes-López, J. A., Ramírez-Hernández, J., Lázaro-Mancilla, O., Carreón-Diazconti, C., Garrido, M. M. L. (2008): Assessment of groundwater contamination by landfill leachate: A case in México. *Waste Manag*., 28, pp. 33–39.

[7] Adeoti, L., Alile, O., Uchegbulam, O. (2009): Geophysical investigation of saline water intrusion into freshwater aquifers: A case study of oniru, Lagos State. *Sci. Res. Essays*, 5, pp. 248–259.

[8] Sikandar, P., Bakhsh, A., Ali, T. (2010): Vertical electrical sounding (VES) resistivity survey technique to explore low salinity groundwater for tubewell installation in Chaj Doab. *J. Agric. Resour*., 48, pp. 547–566.

[9] Cid-Fernandez, J., Araujo, P. (2007): VES characterization of a geothermal area in the NW of Spain. EIEAF *Che* 6, pp. 2173–217.

[10] El-Qady, G. (2006): Exploration of a geothermal reservoir using geoelectrical resistivity inversion: Case study at Hammam Mousa, Sinai, Egypt. *J. Geophys. Eng*., 3, pp. 114–121.

[11] Mazác, O., Cislerova, M., Vogel, T. (1988): Application of geophysical methods in describing spatial variability of saturated hydraulic conductivity in the zone of aeration. *J. Hydrol*., 103, pp. 117–126.

[12] Ojelabi, E., Badmus, B., Salau, A. (2002): Comparative Analysis of Wenner and Schlumberger Methods of Geoelectric Sounding in subsurface delineation and groundwater exploration-a case study. *J Geol Soc India,* 60, pp. 623–628.

[13] Griffiths, D., Barker, R. (1993): Two dimensional resistivity imaging and modeling in areas of complex geology. *J. Appl. Geophys*., pp. 211–226.

[14] Loke, M. H. (2000a): Electrical imaging surveys for environmental and engineering studies: A Practical Guide to 2D and 3D Surveys., 2004, pp. 61. Available on: <www.terrajp.co.Jp/lokenote.pdf>.

[15] Loke, MH. (2000b): *Topographic modelling in electrical imaging inversion* in: Proceedings 62nd Meeting of the European Association of Exploration Geoscientists, Glasgow, Scotland. pp. 1–4.

[16] Collela, A., Lapenna, V., Rizzo, E. (2004): High-resolution imaging of the High Agri Valley Basin (Southern Italy) with electrical resistivity tomography. *Tectonophysics,* 386, pp. 29–40.

[17] Steeples, D. (2001): Engineering and environmental geophysics at the millennium. *Geophysics,* 66, pp. 31–35.

[18] Stone, D., 1994. *Designing Seismic Surveys in Two and Three Dimensions* in: SEG, 244. (* Edited by Charles A. Meeder). Society of Exploration Geophysicists., Tulsa, Oklahoma.

[19] Vermeer, G. J. (2000): *3-D Seismic Survey Design*. Society of Exploration Geophysicists, Tulsa, Oklahoma.

[20] Weimer, P., Davis, T. (1996): *Applications of 3-D Seismic Data to Exploration and Production*, SEG, 270. Society of Exploration Geophysicists, Tulsa, Oklahoma.

[21] Akinmosin, A. A., Omosanya, K. O., Ikhane, P. R., Mosuro, G. O., Adetoso, A. O. (2012): Electrical Resistivity Imaging (ERI) of basin fills in some parts of Eastern Dahomey. *Int. Res. J. Geol. Min*., 2(7), pp. 174-185.

[22] Burke, K. C., Dessauvagie, T. F., Whiteman, A. (1971): The opening of the Gulf of Guinea and Geological History of the Benue Depression and Niger Delta. *Nat. Phys. Sci*., 233, pp. 51–55.

[23] Kingston, D., Dishroon, C., Williams, P. (1983): Global Basin Classification System. *AAPG Bull.,* 67, pp. 2175–2193.

[24] Klemme, H. (1975): *Geothermal Gradients, Heatflow and Hydrocarbon Recovery*., in: A.G. Fischer and S. Judson (eds), Petroleum and Global Tectonics. Princeton Univ. Press, Princeton, New Jersey, pp. 251–304.

[25] Whiteman, A. (1982): *Nigeria: Its Petroleum Geology, Resources and Potential*. Grahan and Trontman, London.

[26] Mpanda, S. (1997): Geological development of east African coastal basin of Tanzania. *Acta Univ*. Stockh. 45, pp. 121.

[27] Storey, B. C. (1995): The role of mantle plumes in continental break-up, case history from Gondwanaland nature. *Nature,* 377, pp. 301–308.

[28] Ekweozor, C., Nwachukwu, J. (1989): The origin of Tar sands in southwestern Nigeria. *NAPE Bull*., 4, pp. 82–84.

[29] Akinmosin, A., Omosanya, K., Ariyo, S., Folorunsho, A., Aiyeola, S. (2011): Structural control for bitumen seepages in imeri, southwestern Nigeria. *International Journal of Basic and Applied Sciences*, 11, 1, pp. 93–103.

[30] Woakes M, Ajibade C. A, Rahaman, M. A. (1987): Some metallogenic features of the Nigerian Basement, *Jour. of Africa Science,* 5 pp. 655-664.

[31] Jones, H., Hockey, R. D. (1964): The Geology of Part of Southwestern Nigeria. *Geol Surv Nig Bull,* 3.

[32] Omatsola, M., Adegoke, O. (1981): Tectonic evolution and Cretaceous stratigraphy of the Dahomey Basin. *J. Min. Geol*., 18, pp. 130–137.

[33] Nton, M. (2001): Aspect of Rock Evaluation Studies of the Maastrichtian-Eocene Sediments. *J. Min. Geol*., 13, pp. 33–39.

[34] Enu, E. (1990): Aspect of Rock Evaluation Studies of the Maastrichtian-Eocene Sediments. *J. Min. Geol*., 40, pp. 29–40.

[35] Nton, M., Elueze, A. (2005): Composition Characteristics and Industrial Assessment of Sedimentary Clay bodies in part of Eastern Dahomey basin, Southwestern Nigeria. *J. Min. Geol*., 4, pp. 175–184.

[36] Agagu, O. K. (1985): *A geological guide to bituminous sediments in Southwestern Nigeria*. Unpubl. Report, Department of Geology, University of Ibadan.

[37] Vouillamoz, J. M., Chatenoux, B., Mathieu, F., Baltassat, J. M., Legchenko, A. (2007): Efficiency of joint use of MRS and VES to characterize coastal aquifer in Myanmar. *J. Appl. Geophys.,* 61, pp. 142–154.

[38] Cardimona, S. (2002): *Electrical resistivity techniques for subsurface investigation*. Dep. Geophys. Univ. Mo. Rolla-Mo.

[39] Loke, M. H., Chambers, J. E., Rucker, D. F., Kuras, O., Wilkinson, P. B. (2013): Recent developments in the direct-current geoelectrical imaging method. *J. Appl. Geophys*., 95, pp. 135–156.

[40] Dahlin, T., Loke, M. H. (1998): Resolution of 2D Wenner resistivity imaging as assessed by numerical modelling. *J. Appl. Geophys.,* 38, pp. 237–249.

[41] Dhakate, R., Singh, V. S., Negi, B. C., Chandra, S., Rao, V. A. (2008): Geomorphological and geophysical approach for locating favorable groundwater zones in granitic terrain, Andhra Pradesh, India. *J. Environ. Manage*., 88, pp. 1373–1383.

[42] Hussein, M. T., Awad, H. S. (2006): Delineation of groundwater zones using lithology and electric tomography in the Khartoum basin, central Sudan. *Comptes Rendus Geosci*., 338, pp. 1213–1218.

[43] Nguyen, F., Garambois, S., Jongmans, D., Pirard, E., Loke, MH. (2005): Image processing of 2D resistivity data for imaging faults. *J. Appl. Geophys*., 57, pp. 260–277.

[44] Ward, S. (1990): Resistivity and induced polarization methods, in: Geotechnical and Environmental Geophysics. Society of Exploration Geophysicists.

[45] Jha, M. K., Kumar, S., Chowdhury, A. (2008): Vertical electrical sounding survey and resistivity inversion using genetic algorithm optimization technique. *J. Hydrol.,* 359, pp. 71–87.

[46] Van Nostrand, Robert, G., Cook, K. (1966): *Interpretation of resistivity data*. U. S. Govt. Print. Off.

[47] Omosanya, K., Mosuro, G., Azeez, L. (2012): Combination of geological mapping and geophysical surveys for surface-subsurface structures imaging in Mini-Campus and Methodist Ago-Iwoye NE Areas, Southwestern Nigeria. *J. Geol. Min. Res.,* 4, pp. 105–117.

[48] Loke, M. H., Barker, R. (1996): Rapid least-squares inversion of apparent resistivity stratigraphic sections by a quasi-Newton method. *Geophys. Prospect*., 44, pp. 131–152.